arXiv:2207.01869v1 [cs.CV] 5 Jul 2022

Distance Matters in Human-Object Interaction Detection

Guangzhi Wang
guangzhi.wang@u.nus.edu
Institute of Data Science, National University of Singapore

Yangyang Guo*
guoyang.eric@gmail.com
School of Computing, National University of Singapore

Yongkang Wong
yongkang.wong@nus.edu.sg
School of Computing, National University of Singapore

Mohan Kankanhalli
mohan@comp.nus.edu.sg
School of Computing, National University of Singapore

ABSTRACT

Human-Object Interaction (HOI) detection has received considerable attention in the context of scene understanding. Despite the growing progress on benchmarks, we realize that existing methods often perform unsatisfactorily on distant interactions, where the leading causes are two-fold: 1) Distant interactions are by nature more difficult to recognize than close ones. A natural scene often involves multiple humans and objects with intricate spatial relations, making the interaction recognition for distant human-object largely affected by complex visual context. 2) Insufficient number of distant interactions in benchmark datasets results in under-fitting on these instances. To address these problems, in this paper, we propose a novel two-stage method for better handling distant interactions in HOI detection. One essential component in our method is a novel Far Near Distance Attention module. It enables information propagation between humans and objects, whereby the spatial distance is skillfully taken into consideration. Besides, we devise a novel Distance-Aware loss function which leads the model to focus more on distant yet rare interactions. We conduct extensive experiments on two challenging datasets – HICO-DET and V-COCO. The results demonstrate that the proposed method can surpass existing approaches by a large margin, resulting in new state-of-the-art performance.

CCS CONCEPTS

• **Computing methodologies** → **Scene understanding**; **Neural networks**; **Spatial and physical reasoning**.

KEYWORDS

Human-Object Interacton Detection, Scene Understanding

ACM Reference Format:
Guangzhi Wang, Yangyang Guo, Yongkang Wong, and Mohan Kankanhalli. 2022. Distance Matters in Human-Object Interaction Detection. In *Proceedings of ACM Conference (Conference'17).* ACM, New York, NY, USA, 9 pages. https://doi.org/10.1145/nnnnnnn.nnnnnnn

*Corresponding Author.

Permission to make digital or hard copies of all or part of this work for personal or classroom use is granted without fee provided that copies are not made or distributed for profit or commercial advantage and that copies bear this notice and the full citation on the first page. Copyrights for components of this work owned by others than ACM must be honored. Abstracting with credit is permitted. To copy otherwise, or republish, to post on servers or to redistribute to lists, requires prior specific permission and/or a fee. Request permissions from permissions@acm.org.
Conference'17, July 2017, Washington, DC, USA
© 2022 Association for Computing Machinery.
ACM ISBN 978-x-xxxx-xxxx-x/YY/MM…$15.00
https://doi.org/10.1145/nnnnnnn.nnnnnnn

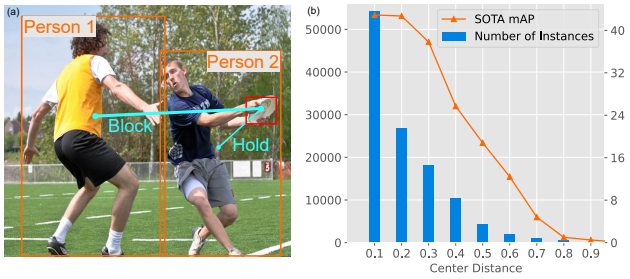

Figure 1: (a) An example of distance influence for interaction prediction. The distant interaction ⟨`person1`, `block`, `frisbee`⟩ is harder to predict than the close one ⟨`person2`, `hold`, `frisbee`⟩. (b) Performance variance of state-of-the-art method UPT [56] and instance numbers with respect to normalized human-object center distances on the HICO-DET dataset [4]. It can be seen that distant interactions are relatively sparse and lead to worse results of UPT.

1 INTRODUCTION

Given a natural image, the task of Human-Object Interaction (HOI) detection is to localize all humans and objects, and recognize the interaction between each human-object pair. It constitutes an important step towards high-level scene understanding, and has benefited many multimedia applications, including visual question answering [2, 13], image captioning [45] and surveillance event detection [1].

This task is by its nature challenging, as visual recognition and spatial relation understanding are both required. Existing efforts can be mainly categorized as two-stage and one-stage methods based on their detection strategy. Two-stage methods [4, 10, 11, 51] initially employ an off-the-shelf detector (*e.g.*, Faster R-CNN [38]) to detect all humans and objects in the image. Thereafter, the detected humans and objects are exhaustively paired, followed by another network for interaction classification. By contrast, one-stage methods [21, 27, 57] attempt to solve this problem in a single stage. In particular, with the success of the Transformer [44] architecture, many approaches [22, 41, 54, 58] adopt the attention-based DETR [3] framework in HOI detection and have achieved better performance than their two-stage counterparts. However, the slow convergence of DETR results in high memory cost and increasing training overhead. By this reason, Zhang *et al.* [56] proposed to revitalize two-stage approaches with the help of DETR. For this

method, the object detection is achieved with a fixed DETR in the first stage, and another attention-like mechanism is adopted for predicting the interactions.

In fact, performing interaction recognition expects accurate understanding about the spatial relation between human and objects, where the distance serves as one fundamental characteristic. Nevertheless, predicting interactions with different human-object distances is of distinct difficulties. Take Fig. 1 (a) as an example, the distant interaction ⟨`person1`, `block`, `frisbee`⟩ is harder to recognize than ⟨`person2`, `hold`, `frisbee`⟩, even for us humans. This observation is further reflected in Fig. 1 (b), where state-of-the-art method UPT [56] performs much worse on distant interactions. We attribute this problem to two inherent reasons. Firstly, distant interactions are intrinsically more difficult to recognize, owing to the scene complexity. A natural image often includes multiple humans and objects, while some of them overlap and entangle with each other. As a result, predicting interaction for distant human-object pairs is largely affected by their noisy context. Furthermore, distant interactions usually involve small objects, on which the detection backbone struggles due to low-resolution and occlusion. Secondly, the number of interactions with respect to human-object center distance demonstrates a long-tail distribution (see Fig. 1 (b)). Thus, it is unfavorable to fit distant human-object pairs in the training process, resulting in sub-optimal performance. Nevertheless, to the best of our knowledge, such an important problem remains unexplored by the HOI detection literature.

In this paper, we make contributions from the following two aspects to address the aforementioned problem. Firstly, we shed light on the two-stage training scheme in HOI detection and propose a novel two-stage method, dubbed Spatially Differentiated Transformer (SDT). Inspired by [56], we employ DETR to detect humans and objects (*i.e.* tokens), the representations of which are then enriched via an intra-class diversification module and spatial fusion. Then, we design a novel Far-Near Distance Attention (FNDA) mechanism to enable improved modeling for distant token pairs. Specifically, FNDA allows one token to propagate information with two glances: the first glance involves only far away tokens while the second glance focuses solely on near tokens. In this way, the model is able to better attend to distant tokens without the influence of nearby ones and vice versa. Thereafter, we pair the obtained features of each human and object, and employ another self-attention module for iterative context aggregation. At last, each human-object pair is classified into candidate interactions.

Furthermore, as the number of interactions manifests a long-tail distribution with respect to human-object distances, we therefore design a novel Distance-Aware (DA) loss function to re-weight each human-object pair during training. In particular, DA loss adaptively adjusts the weights for each human-object pair, wherein relatively higher and lower weights are assigned to distant and close interactions, respectively. It is expected that with our DA loss, distant interactions are treated with more importance, thereby alleviating the effect of dominance of close interactions during training.

To validate the effectiveness of our proposed method, we conduct extensive experiments on two challenging benchmarks, namely HICO-DET [4] and V-COCO [15]. The results show that our method outperforms existing approaches by a large margin, resulting in new state-of-the-art performance on the two benchmarks. Besides, additional analysis and visualizations further demonstrate that our method is able to better model distant interactions.

To summarize, the contributions of this paper are three-fold:

- We propose a novel two-stage method – Spatially Differentiated Transformer for HOI detection, wherein a Far-Near Distance Attention (FNDA) is devised to effectively model distant interactions.
- To balance the learning of interactions with different human-object distances, we design a novel Distance-Aware (DA) loss function to dynamically adjust the weight of each human-object pair according to their center distance.
- Extensive experiments on two benchmarks demonstrate that the proposed method surpasses existing approaches by a large margin, achieving new state-of-the-art results[1].

2 RELATED WORK

2.1 Human-Object Interaction Detection

Existing approaches for HOI detection can be mainly categorized as two-stage and one-stage methods, according to their detection strategy. Two-stage methods firstly adopt an off-the-shelf detector (like Faster-RCNN [38]) to detect all humans and objects in the image. Afterwards, the humans and objects are exhaustively paired and fed into a downstream network for interaction recognition. These approaches mostly focus on improving the interaction recognition capacity of the downstream network. Early work [4, 40] often leverages the visual appearance and spatial relation to identify the interactions. In addition, more features such as human pose [16, 46], gaze [50], 3D representations [24] and word embeddings [23, 32], have also been exploited. Different from these methods, some studies utilize the graph structure for information propagation between the detected humans and objects. For example, [36] builds a fully-connected graph while [10, 55] apply a bipartite graph for humans and objects. Despite their effectiveness, these methods usually suffer from sub-optimal detection performance [10, 25, 55].

By contrast, one-stage methods tackle the task in an end-to-end manner. Early one-stage approaches often detect the interaction points [27, 47] or the human-object union regions [21] as interaction clues. Recently, with the success of DETR in the object detection domain, some studies attempt to employ this Transformer-based architecture for HOI detection. For instance, [22, 41, 58] append more heads on the decoder to recognize the interaction. [6] applies another decoder for decoupled object detection and interaction recognition, while [54] performs the two steps in a cascaded way.

2.2 Single- and Cross-Modal Attention

The past few years have witnessed the rapid development of attention mechanism due to its effectiveness in a variety of tasks. Among the dedicated efforts, the Multi-Head Self-Attention (MHSA) [44] has recently attracted increasing research interest. In addition to its wide application in the language domain, some researchers attempt to apply MHSA to the vision tasks, such as image classification [7], semantic segmentation [33], point cloud analysis [8, 9] and video understanding [35]. Besides, some studies have been conducted to

[1]Code available: https://github.com/daoyuan98/SDT-HOI.

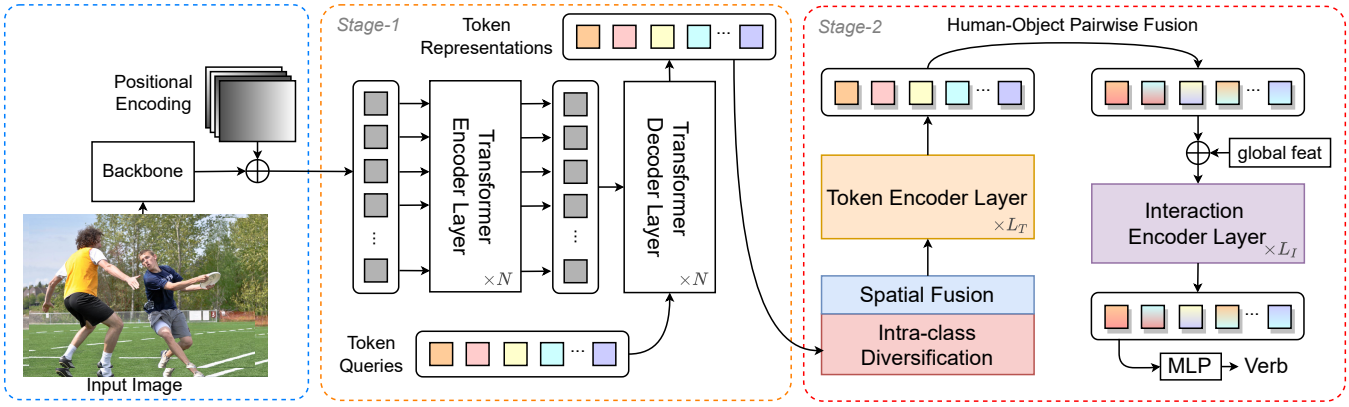

Figure 2: Illustration of the proposed Spatially Differentiated Transformer (SDT). Given a natural image, a backbone network is employed to extract a set of visual features. After added with the positional encodings, we adopt DETR [3] to detect all tokens, *i.e.*, humans and objects. The token representations are fed into an Intra-Class Diversification module and a spatial fusion module to enrich the interaction information. Then, we employ L_T Token Encoder Layers to propagate information between tokens. After that, each human-object pair is fused with the global visual feature, and inputted into L_I Interaction Encoder Layers for iterative context aggregation. Finally, an Multi-Layer Perceptron (MLP) is used for interaction prediction.

improve the efficiency of the attention mechanism. For example, [5, 14, 48] present to reduce the computational cost or model bi-level relations by splitting attention into two groups of different receptive fields. Qin *et al.* [37] decreases the quadratic computation complexity by eliminating the softmax layer. Other methods also consider the relative position between inputs by taking it as learned relative bias embedding [39] or part of the attention weights [33, 48]. While above methods focus only on single modality information, the effectiveness of the attention mechanism on cross-modality tasks has also been extensively studied. One typical operation is to replace the query matrix with the features from another modality, and the cross-modality information exchange is accordingly enabled. It demonstrates improved results on various multi-modal tasks, including visual question answering [31], image-text matching [30, 49], zero-shot learning [52] and audio-visual active speaker detection [42].

3 METHODOLOGY

3.1 Preliminary

Method Intuition. Human-Object Interaction (HOI) detection is to detect and predict a set of ⟨human, verb, object⟩ interaction triplets in an image. In this work, we attempt to address the problem that distant human-object often lead to inferior interaction recognition results. In particular, we propose a novel two-stage method named Spatially Differentiated Transformer (SDT), which is designed to flexibly model both distant and close interactions. As shown in Fig. 2, our method is composed of two stages: The first stage detects human and object (token) with an object detector, followed by the second stage of interaction recognition on the detected tokens.

Stage 1: Token Detection. Inspired by [56], we perform token detection with a Transformer-based DETR [3], which demonstrates superior results in object detection. In this step, an input image is first fed into a backbone network, *e.g.*, ResNet-50 [17], to obtain the visual representation $\boldsymbol{g} \in \mathbb{R}^d$. With the addition of positional encodings, the visual features are then inputted to N Transformer encoder layers and N Transformer decoder layers sequentially. Thereafter, we have a set of token representations, corresponding to the token queries inputted to the decoder layers. Finally, these token representations are fed into two separate Multi-Layer Perceptrons (MLPs) for object classification and bounding box regression, respectively.

Stage 2: Interaction Recognition. In the second stage, we filter the tokens according to their confidence scores, and keep n most confident ones. Each token is represented as a feature vector $\boldsymbol{t}_i \in \mathbb{R}^d$, normalized bounding box $\boldsymbol{b}_i \in \mathbb{R}^4$, confidence score s_i, and class c_i, where $i = 1, ..., n$. With the detected tokens, we first post-process these tokens to make them more compatible with HOI detection. Then, these tokens are enabled to propagate information with distance discrimination by our Far-Near Distance Attention. Afterwards, we obtain the interaction representation by combing each human and object tokens with the global context. Finally, the interaction representations are fed into an MLP for final prediction. In the rest of this section, we will sequentially elaborate the token post-processing step, the Far-Near Distance Attention, our Distance-Aware loss function, and training and inference procedures.

3.2 Token Post-Processing

The token representations $\{\boldsymbol{t}_i\}_{i=1}^n$ obtained from DETR contains discriminative information for classification. However, they can be of low quality and oblivious to the spatial relations with other tokens. Therefore, we first post-process these tokens to enrich their representation for better interaction recognition.

Intra-Class Diversification. It is reasonable that the token representations are often of limited diversity. In particular, tokens

representing small size objects often suffer from occlusion and low-resolution due to the scene complexity, and is thus less informative. To this end, we propose an Intra-Class Diversification (ICD) module to enrich the token representations with the help of other instances from the same class.

The key to our ICD module is an object-wise memory, which stores token representations of high confidence score for each class. During training, given a token with representation $\boldsymbol{t}_i$, we take it as a query and randomly sample l features $\{\boldsymbol{t}_k\}_{k=1}^{l}$ from the memory cell corresponding to its class for key and value computation. Then, the intra-class diversification is implemented through the cross-attention mechanism [44]:

$$\begin{cases} \boldsymbol{A}_{ik} & = & \frac{\boldsymbol{t}_i \boldsymbol{W}_Q \boldsymbol{W}_K^T \boldsymbol{t}_k^T}{\sqrt{d}} \\ \boldsymbol{B}_{ik} & = & \frac{e^{\boldsymbol{A}_{ik}}}{\sum_{k'=1}^{l} e^{\boldsymbol{A}_{ik'}}} \\ \tilde{\boldsymbol{t}}_i & \leftarrow & \boldsymbol{t}_i + \sum_{k'=1}^{l} \boldsymbol{B}_{ik'} \boldsymbol{t}_{k'} \boldsymbol{W}_V \end{cases} \tag{1}$$

where $\boldsymbol{W}_Q, \boldsymbol{W}_K, \boldsymbol{W}_V \in \mathbb{R}^{d \times d}$ are learnable transformation matrices. This mechanism allows each token to adaptively aggregate representation from high quality tokens in the same class, thereby improving token diversity and enhancing model's generalizability.

Spatial Fusion. Besides the visual representation, the bounding box of a detected token also serves as a key attribute for describing the spatial information. For understanding the relation between two tokens, it is more important to focus their relative spatial relations. Thus, inspired by [55, 56], we first obtain the pairwise spatial relation $\boldsymbol{p}_i = f(\boldsymbol{b}_i, \{\boldsymbol{b}_j\}_{j=1}^{n})$, which represents the spatial relation between the i-th and all the other tokens[2]. The spatial relation vector $\boldsymbol{p}_i$ can be regarded as a high-level positional embedding, which better represents the detected tokens. Afterwards, we fuse the pairwise spatial relation $\boldsymbol{p}_i$ into the token representations:

$$\hat{\boldsymbol{t}}_i = \mathsf{FFN}([\tilde{\boldsymbol{t}}_i; \boldsymbol{p}_i]), \tag{2}$$

where FFN denotes a feed forward network. With the combination of spatial relations, the processed tokens are more informative, and thus more compatible for HOI detection.

3.3 Far-Near Distance Attention

After fusing the spatial embeddings, one common way to propagate information between tokens is to leverage the Multi-Head Self-Attention (MHSA) mechanism in Transformer [44]. Nonetheless, it is sub-optimal to directly apply MHSA for HOI detection. Broadly speaking, one human can interact with multiple objects and vice versa, making MHSA struggle on dense scenes. Furthermore, interaction prediction for tokens with far and near distances is often of distinct difficulties. Current MHSA tackles all token-pairs without discrimination, which may unexpectedly impede the modeling for distant relations.

To this end, we design a novel Far-Near Distance Attention (FNDA) mechanism, which models the relation between tokens in two alternative steps, according to their center distance. Specifically, given the bounding boxes of the detected tokens, we first compute

[2]We detail the computation of f in supplementary material due to space limit.

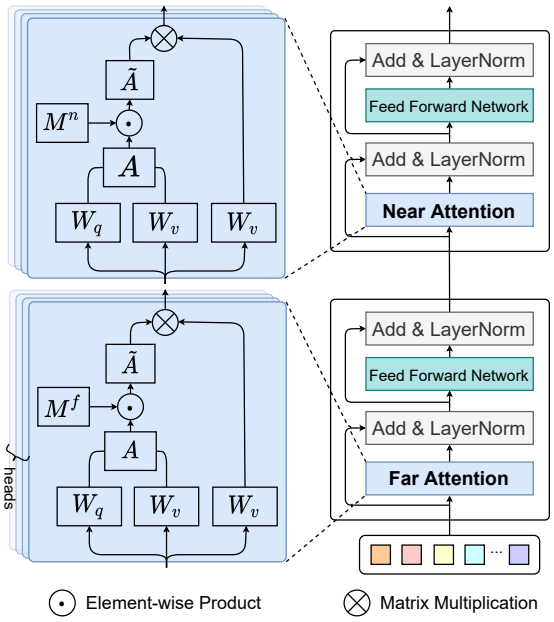

Figure 3: Each token encoder layer contains two blocks, where far attention mask $\boldsymbol{M}^f$ and near attention mask $\boldsymbol{M}^n$ are alternatively applied. Note that the softmax operation is folded for clarity.

L_2 center distance for each token pair, and obtain the pairwise distance matrix $\boldsymbol{D} \in \mathbb{R}^{n \times n}$. Afterwards, we compute two attention masks $\boldsymbol{M}^f$ and $\boldsymbol{M}^n$ as follows:

$$\begin{aligned} \boldsymbol{M}_{ij}^f &= \begin{cases} 1, & \boldsymbol{D}_{ij} > Med(\boldsymbol{d}_i) \ or \ i = j \\ 0, & otherwise \end{cases} \\ \boldsymbol{M}_{ij}^n &= \begin{cases} 1, & i = j \\ 1 - \boldsymbol{M}_{ij}^f, & otherwise \end{cases}, \end{aligned} \tag{3}$$

where $Med(\boldsymbol{d}_i)$ denotes the median of the i-th row in matrix $\boldsymbol{D}$, which serves as the threshold for differentiating far and near distances. In this way, $\boldsymbol{M}^f$ allows the model to attend to far tokens only, which prohibits the intervention from near ones, and vice versa[3]. Then, we perform the MHSA operation with the distance-guided masks:

$$\begin{cases} \boldsymbol{A}_{ij} & = & \frac{\hat{\boldsymbol{t}}_i \boldsymbol{W'}_Q \boldsymbol{W'}_K^T \hat{\boldsymbol{t}}_j^T}{\sqrt{d}} \\ \tilde{\boldsymbol{A}} & = & \boldsymbol{A} \odot \boldsymbol{M}^{f|n} \\ \boldsymbol{B}_{ik} & = & \frac{e^{\tilde{\boldsymbol{A}}_{ik}}}{\sum_{k'=1}^{n} e^{\tilde{\boldsymbol{A}}_{ik'}}} \\ \tilde{\boldsymbol{t}}_i & \leftarrow & \tilde{\boldsymbol{t}}_i + \sum_{k'=1}^{k} \boldsymbol{B}_{ik'} \boldsymbol{t}_{k'} \boldsymbol{W'}_V \end{cases} \tag{4}$$

where $\odot$ denotes element-wise product, $\boldsymbol{W'}_Q, \boldsymbol{W'}_K, \boldsymbol{W'}_V \in \mathbb{R}^{d \times d}$ are learnable transformation matrices , $\boldsymbol{M}^{f|n}$ indicates either $\boldsymbol{M}^f$ or $\boldsymbol{M}^n$. In our model, $\boldsymbol{M}^f$ and $\boldsymbol{M}^n$ are alternatively applied, so that each token can iteratively update their representations with tokens

[3]Note that the diagonal elements are not masked in $\boldsymbol{M}^f$ and $\boldsymbol{M}^n$ so that one token can always attend to itself.

of different distances, thereby improving the model's capacity for distant relation modeling. It is worth noting that our FNDA can replace MHSA in the Transformer encoder layer with few efforts, resulting in our token encoder layer. The detailed operation is illustrated in Fig. 3.

Iterative Context Aggregation. Thereafter, we pair each human token and object token, and take them as the initial interaction representation for each candidate pair. We also fuse the global context feature $\boldsymbol{g}$ into the representations, which can provide contextual clues for interaction recognition:

$$\boldsymbol{h}_{ij} = [\tilde{\boldsymbol{t}}_i; \tilde{\boldsymbol{t}}_j] \oplus \mathsf{FFN}(\boldsymbol{g}), \tag{5}$$

where $\oplus$ denotes element-wise addition, i implies the index for human and $i \neq j$. We then employ L_I interaction encoder layers to perform self-attention [44] to iteratively update the interaction representations with the global context. After that, an MLP is used to predict the final interactions for each human-object pair.

3.4 Distance-Aware Loss

Following previous work [4, 32, 54, 55], we formulate interaction recognition with an multi-label classification objective, since there can be multiple interactions (*e.g.*, `read book` and `hold book`) within one human-object pair. In this way, the full model can be optimized with the Binary Cross Entropy (BCE) loss. However, distant interactions often manifest rare in benchmark datasets, which leads to underfitting on these interactions. Therefore, we propose a Distance-Aware (DA) loss to adaptively assign higher weights and lower weights to distant and close interactions, respectively. In formulation, the interaction recognition model is optimized with:

$$\mathcal{L}_{DA} = \sum_{i,j\ i\neq j} w_{ij} \sum_{c\in C} \boldsymbol{y}_{ij}^c log\boldsymbol{\delta}_{ij}^c + (1-\boldsymbol{y}_{ij}^c) log(1-\boldsymbol{\delta}_{ij}^c), \tag{6}$$

where $\boldsymbol{\delta}_{ij} = \sigma(\mathsf{MLP}(\boldsymbol{h}_{ij}))$ represents the verb scores transformed by the sigmoid function $\sigma(\cdot)$, C is the number of classes and $\boldsymbol{y}_{ij}^c$ indicates the ground-truth label of class c. We implement w_{ij} as,

$$w_{ij} = \sigma(\alpha \cdot \boldsymbol{D}_{ij} + \beta), \tag{7}$$

where $\boldsymbol{D}_{ij}$ is the L_2 center distance between the i-th human and the j-th object, and α and β are both learnable parameters. In this way, relatively higher weights are assigned to more distant interactions, so as to increase their importance during training. Notably, the proposed DA loss acts on each instance.

3.5 Training and Inference

Training. We first train the object detector, and then freeze it to train the interaction recognition model. Pertaining to the latter training phase, focal loss [28] has been proven effective to tackle the class-imbalance problem, which is shown to be influential to the performance in HOI detection [19, 55, 56]. Therefore, we combine our DA loss with the focal loss to optimize our model. Besides, since our method breaks HOI detection into two stages, after detection, infeasible verb-object combinations can be filtered out in advance.

Inference. During inference, the final interaction score $\boldsymbol{z}$ is calculated as the multiplication of human confidence score s_i, object confidence score s_j and their verb score $\boldsymbol{\delta}_{ij}^c$:

$$\boldsymbol{z}_{ij}^c = (s_i)^\lambda \cdot (s_j)^\lambda \cdot \boldsymbol{\delta}_{ij}^c, \tag{8}$$

where s_i and s_j are obtained from DETR and $\lambda \geq 1$ is a constant to suppress overconfident objects [55, 56]. Infeasible verb-object combinations are also removed according to the object label output by DETR.

4 EXPERIMENTS

4.1 Experimental Setup

Datasets. We conducted experiments on two benchmark datasets, namely HICO-DET [4] and V-COCO [15]. **HICO-DET** involves 80 COCO objects and 117 verb classes, resulting in a total of 600 interaction classes. There are 38,118 and 9,658 images for training and test in this dataset, respectively. **V-COCO** is built upon the MS-COCO [29] dataset. It covers 24 action categories with 80 COCO objects, and contains 2,533, 2,867 and 4,946 images for training, validation and test, respectively.

Evaluation Protocol. We adopted mean Average Precision (mAP) as the evaluation metric. A detection result is regarded as true positive if (1) the predicted human and object bounding box have IoUs larger than 0.5 with corresponding ground-truth boxes, and (2) the predicted action class is correct. We computed this metric for each interaction class in HICO-DET and verb class in V-COCO.

Following [4, 54, 56], we provide results under *default setting* and *known-object setting* on HICO-DET. For the first setting, the APs are calculated on the basis of all test images, while the second setting calculate APs based on images that contain the object corresponding to each class. Under both settings, the result under *full* (a total of 600 interaction classes), *rare* (less than 10 training instances) and *non-rare* (10 or more training instances) classes are all reported.

For V-COCO, we provide results under two evaluation settings: *Scenario 1* and *Scenario 2*. In the former setting, the detector is required to report an empty box when no object is involved in the interaction, while the object box can be ignored in the latter one.

Implementation Details. We first fine-tuned DETR for 30 epochs on the two datasets, which has been pre-trained on MS-COCO[4]. Following [56], some data augmentation techniques were applied in the detector fine-tuning process: We scaled the images such that the shorter side is between 480 to 800 pixels while the longer side is at most 1,333 pixels. Furthermore, each image was cropped with a probability of 0.5 to a random rectangle with each side between 384 to 600 pixels before scaled. Besides, we also applied color jittering augmentation, where brightness, contrast and saturation are randomly selected between 0.6 to 1.4. After that, the DETR was frozen in the next stage for interaction recognition.

For each given image, the fine-tuned DETR first perform object detection and generate 100 proposals. Then, we filter out tokens with confidence score less than 0.2, and keep 3~15 human/object tokens with higher confidence, based on which our SDT is trained. We trained the interaction recognition model with the AdamW optimizer [34], which has a learning rate of 2e-4 and weight decay of 1e-4. The SDT is trained for 20 epochs and the learning rate is decayed by 10 at the 10-th epoch. L_T was set to 3 on both datasets

[4]Note that MS-COCO training set contains some images in the V-COCO test set, which should be excluded in the detector pre-training process [41, 56].

Table 1: Results on the HICO-DET and V-COCO datasets. The best results are highlighted in bold while the second best ones are underscored.

	HICO-DET						V-COCO	
	Default Setting			Known-Object Setting				
Method	Full	Rare	Non-rare	Full	Rare	Non-rare	Scenario 1	Scenario 2
HO-RCNN [4]	7.81	5.37	8.54	10.41	8.94	10.85	-	-
InteractNet [12]	9.94	7.16	10.77	-	-	-	40.0	-
GPNN [36]	13.11	9.34	14.23	-	-	-	44.0	-
TIN [26]	17.03	13.42	18.11	19.17	15.51	20.26	47.8	54.2
DRG [10]	19.26	17.74	19.71	23.40	21.75	23.89	51.0	-
VSGNet [43]	19.80	16.05	20.91	-	-	-	51.8	57.0
DJ-RN [24]	21.34	18.53	22.18	23.69	20.64	24.60	-	-
PPDM [27]	21.94	13.97	24.32	24.81	17.09	27.12	-	-
ConsNet [32]	22.15	17.55	23.52	-	-	-	53.2	-
VCL [18]	23.63	17.21	25.55	25.98	19.12	28.03	48.3	-
ATL [19]	23.81	17.43	27.42	-	-	-	-	-
IDN [25]	24.58	20.33	25.86	27.89	23.64	29.16	53.3	60.3
HOTR [22]	25.10	17.34	27.42	-	-	-	55.2	64.4
FCL [20]	25.27	20.57	26.67	27.71	22.34	28.93	52.4	-
HOI-Trans [58]	26.61	19.15	28.84	29.13	20.98	31.57	52.9	-
AS-Net [6]	28.87	24.25	30.25	31.74	27.07	33.14	53.9	-
SCG [55]	29.26	24.61	30.65	32.87	27.89	34.35	54.2	60.9
QPIC [41]	29.90	23.92	31.69	32.38	26.06	34.27	58.8	61.0
OCN [53]	30.91	25.56	32.51	-	-	-	-	-
CDN [54]	31.44	**27.39**	32.64	34.09	**29.63**	35.42	**61.7**	63.8
UPT [56]	**31.66**	25.94	**33.36**	**35.05**	29.27	**36.77**	59.0	**64.5**
SDT (ResNet-50)	32.45	28.09	33.75	35.95	31.30	37.34	60.3	65.7
SDT (ResNet-101)	**32.97**	**28.49**	**34.31**	**36.32**	**31.90**	**37.64**	**61.8**	**67.6**

while L_I was 2 and 3 on V-COCO and HICO-DET, respectively. We set λ in Eq. 8 to 1 for training and 2.8 for inference. The token dimension d is set to 256. For all of the attention mechanism adopted in this paper, we set the number of heads to 8, hidden dimension to 1024 and dropout probability to 0.1. We conducted all experiments on 4 NVIDIA RTX A5000 GPUs with CUDA 11.1, whereby each GPU has a batch of 4 images, resulting in an effective batch size of 16. It takes about 6 hours and 40 minutes to train on HICO-DET and V-COCO, respectively. Besides, we employed two backbone networks, *i.e.*, ResNet-50 and ResNet-101 for global feature extraction, resulting in two variants of SDT.

4.2 Comparison with State-of-the-art Methods

We compared the proposed SDT with state-of-the-art methods, and reported the results in Table 1. It can be observed that, with ResNet-50 as backbone, the proposed method already outperforms existing methods significantly on the two datasets. For example, on HICO-DET, we surpass UPT [56] by about 1 mAP on both *default setting* and *known-object setting*. On V-COCO, SDT also achieves consistent improvements. Specifically, under *scenario 1*, our method can outperform the second-best two-stage method UPT [56] by 1.3 mAP, while under *scenario 2*, SDT achieves the best performance over all the existing methods. Notably, the proposed method can also benefit from a stronger backbone (*i.e.*, ResNet-101). For example, on V-COCO, we outperform all existing methods under two scenarios. In particular, under *scenario 2*, we can further improve upon SDT with ResNet-50 by 1.9 mAP, resulting in an improvement of 3.1 mAP upon the runner-up. These results prove the superiority of the proposed method over existing approaches.

4.3 Ablation Studies

To further investigate the effects of each component in the proposed method, we conducted extensive ablation studies on the larger HICO-DET dataset with ResNet-50 as backbone.

Module Effectiveness. We first study the effectiveness of token encoder layers (**T**-Encoder), interaction encoder layers (**I**-Encoder) and DA loss, and show the results in Table 2. We can see that all three modules improve the baseline with a clear margin. For example, with **T**-Encoder, our method surpasses the baseline by more than 2 mAP. Furthermore, any combination of two modules outperforms the variant with a single module, indicating that the modules are in fact complementary to each other. In particular, the combination of **T**-Encoder and **I**-Encoder can boost upon the baseline by more than 4 mAP. Finally, with all of the three modules, the proposed method achieves the best results, which leads to an improvement of more than 5 mAP upon the baseline.

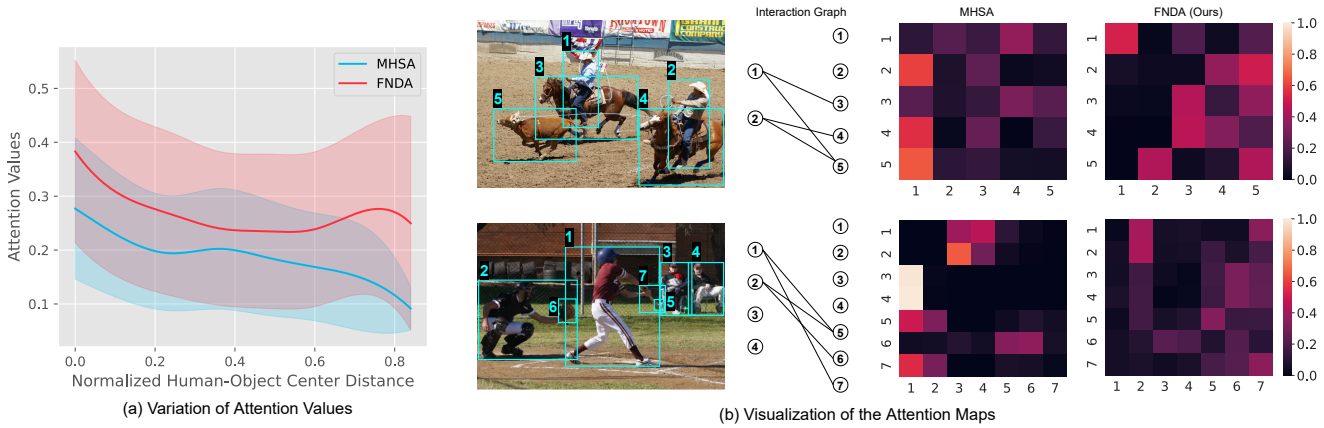

(a) Variation of Attention Values

(b) Visualization of the Attention Maps

Figure 4: Qualitative results from MHSA and the proposed FNDA. (a) Attention value variation of MHSA and FNDA with respect to the normalized center distances. Note that we split the attention values into bins of 0.05 according to the center distance, where the mean and variance in each bin are both shown. (b) Visualization of attention maps in two randomly selected images. The edges in the interaction graphs indicate the existence of interaction between connected nodes.

Table 2: Effectiveness of each module in the proposed SDT.

T-Encoder	**I**-Encoder	DA Loss	Full	Rare	Non-Rare
			27.08	23.01	28.30
✓			29.09	25.06	30.29
	✓		30.04	25.32	31.45
		✓	28.09	24.04	29.29
✓	✓		31.16	26.95	32.42
✓		✓	30.92	27.08	32.07
	✓	✓	30.44	25.92	32.05
✓	✓	✓	**32.45**	**28.09**	**33.75**

Table 3: Performance variation with different numbers of layers.

L_T	L_I	Full	Rare	Non-rare
2	2	31.06	25.98	32.58
2	3	31.40	26.73	32.79
2	4	31.02	25.77	32.59
3	2	31.71	26.95	33.13
3	3	**32.45**	**28.09**	**33.75**
3	4	31.93	27.54	33.24
4	2	30.91	25.01	32.67
4	3	30.82	26.08	32.23
4	4	30.67	25.57	32.20

Number of Layers. We studied the effects of the number of token encoder layers L_T and interaction encoder layers L_I, and show the results in Table 3. It can be observed that the combination of 3 token encoder layers and 3 interaction encoder layers leads to the best performance. Increasing L_T or L_I results in less favorable results, while a smaller L_t or L_I also degrades the model performance due to the underfitting problem.

Table 4: Comparison between MHSA and FNDA. ++ICD means composing ICD upon spatial fusion.

Variant	Full	Rare	Non-Rare
MHSA [44]	30.66	26.06	32.03
+ Spatial Fusion	30.80	24.78	32.60
++ ICD	30.90	26.74	32.14
FNDA (Ours)	31.70	26.26	33.32
+ Spatial Fusion	32.10	27.02	33.62
++ ICD	**32.45**	**28.09**	**33.75**

Quantitative Study on FNDA. To demonstrate the superiority of the proposed FNDA, we compared it with the most widely used Multi-Head Self-Attention (MHSA) [44], and show the results in Table 4. We can see that the plain FNDA exceeds MHSA by more than 1 mAP. In addition, MHSA also benefits from the token post-processing steps, *i.e.*, ICD and spatial fusion, which also proves the validity of these two. After combing our FNDA with these two steps, the performance can be further promoted, making it outperform the MHSA by more than 1.5 mAP.

Qualitative Analysis on FNDA. We used all interactive token pairs in the HICO-DET test set, and kept their corresponding attention values in the token encoder layers for both MHSA and our FNDA. We then illustrate these values with respect to normalized human-object center distances in Fig. 4 (a). It can be observed that the attention values generally decline with the increase of distance for both types of attentions, implying that information propagation between distant pairs is more challenging. More importantly, our FNDA assigns higher attention weights on distant interactions than MHSA, which further justifies the superiority of FNDA over MHSA.

We then used two randomly selected cases to illustrate why FNDA outperforms MHSA. The two images in Fig. 4 (b) are selected from HICO-DET test set and the attention map is averaged for far-attention and near-attention. We observe that the strength

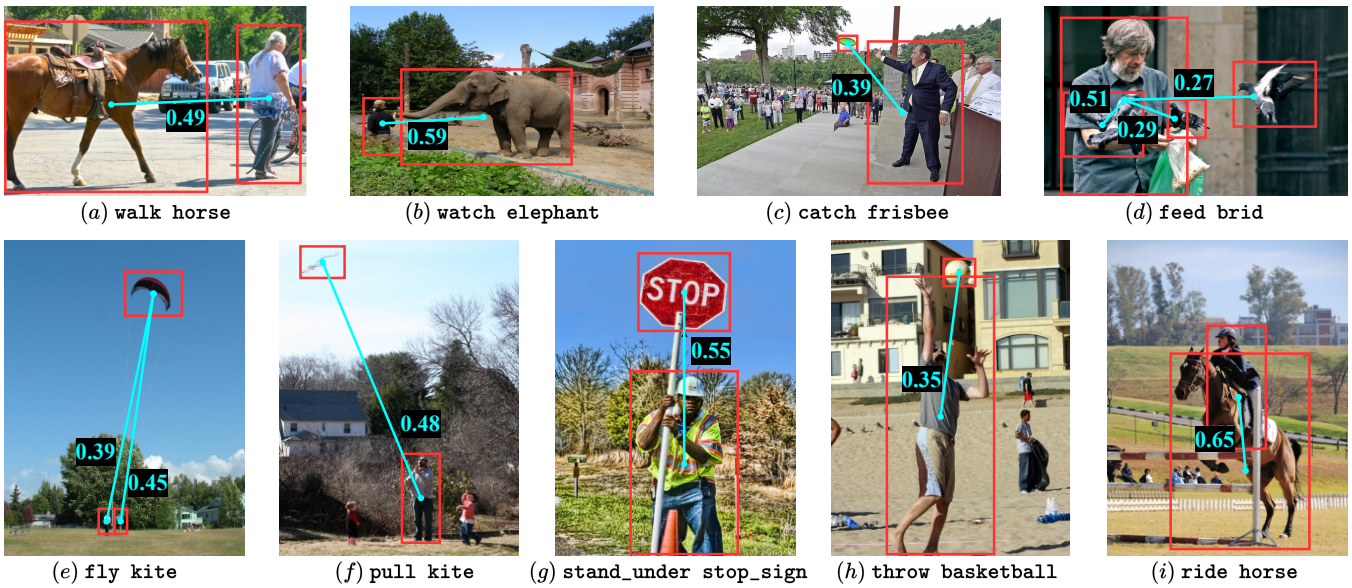

(a) walk horse (b) watch elephant (c) catch frisbee (d) feed brid

(e) fly kite (f) pull kite (g) stand_under stop_sign (h) throw basketball (i) ride horse

Figure 5: Qualitative results from HICO-DET test set. The number adjacent to the line indicates the predicted score of the target interaction. Note that only partial involved human-object interactions are shown for better clarity. Best view in color.

of FNDA comes from two aspects: 1) It can effectively propagate information between distant and interactive human-object pairs, and thus benefit distant interaction recognition. For example, in the first case of Fig. 4 (b), the person in box2 is `lassoing` the `cow` in box5. The attention value (2, 5) is minor in MHSA due to the far distance. By contrast, our FNDA can emphasize more on this human-object pair. 2) FNDA is able to constrain non-interactive human/objects, thereby focusing more on informative ones. For instance, in the second case of Fig. 4 (b), the people in box3 and box4 are not involved in any interactions to the people in box1 and box2. Nonetheless, MHSA assigns higher values in (1, 3), (1, 4), (2, 3), (2, 4), which distracts the people in box1 and box2 from attending to truly related objects. On the contrary, our FNDA can alleviate this problem by attending to more informative tokens in the image.

4.4 Qualitative Results

To further understand the effectiveness of the proposed SDT, we randomly selected some images from the HICO-DET test set and visualized SDT prediction results in Fig. 5. Note that we only showed partial interactions for clearer view. It can be observed that our method is capable of handling interaction of diverse distances. For example, distant instances, such as `fly kite` in Fig. 5 (e) and `pull kite` in Fig. 5 (f), and close instances, such as `ride horse` in Fig. 5 (i), can both be successfully recognized by the proposed method. Notably, when the detected object is small (*e.g.*, the `frisbee` in Fig. 5 (c) and the `ball` in Fig. 5 (h)), SDT can provide the correct interaction with a high confidence. Furthermore, it also demonstrates an evident advantage on scenes with complex context, where multiple objects interact with the same person. For instance, the `man` in Fig. 5 (d) is `feeding` three `birds` simultaneously, yet our method correctly predicts the interaction for all these three objects.

5 CONCLUSION AND FUTURE WORK

In this work, we propose a novel two-stage method for better modeling distant interactions in HOI detection. Two fundamental components make our method distinguished from existing approaches. First, we design a Far-Near Distance Attention to guide the model attention to flexibly focus on distant and close interactions. Second, a novel Distance-Aware loss is presented by this paper to handle the long-tailed interaction-distance distribution. We conduct extensive experiments on two benchmark datasets and observe that our method achieves a new state-of-the-art on them. Additional analysis further validates that the performance gain is mainly brought by the distant interaction modeling from the proposed method.

As indicated by our empirical findings, a large quantity of distant interactions involve relatively small objects, which impedes the interaction recognition due to the weak detection results. It is thus promising for HOI detection to be equipped with improved detectors on small-sized objects. In addition, the 2D image shows limitation in distance estimation as the human-object relations are physically expressed in the 3D world. In view of this, incorporating the depth information to distance modeling will potentially benefit the learning of distant interactions in HOI detection.

ACKNOWLEDGEMENT

This research is supported by the National Research Foundation, Singapore under its Strategic Capability Research Centres Funding Initiative. Any opinions, findings and conclusions or recommendations expressed in this material are those of the author(s) and do not reflect the views of National Research Foundation, Singapore.

REFERENCES

[1] Amit Adam, Ehud Rivlin, Ilan Shimshoni, and Daviv Reinitz. 2008. Robust real-time unusual event detection using multiple fixed-location monitors. *IEEE TPAMI* (2008).

[2] Stanislaw Antol, Aishwarya Agrawal, Jiasen Lu, Margaret Mitchell, Dhruv Batra, C Lawrence Zitnick, and Devi Parikh. 2015. VQA: Visual question answering. In *ICCV*.

[3] Nicolas Carion, Francisco Massa, Gabriel Synnaeve, Nicolas Usunier, Alexander Kirillov, and Sergey Zagoruyko. 2020. End-to-end object detection with transformers. In *ECCV*.

[4] Yu-Wei Chao, Yunfan Liu, Xieyang Liu, Huayi Zeng, and Jia Deng. 2018. Learning to detect human-object interactions. In *WACV*.

[5] Chun-Fu Chen, Rameswar Panda, and Quanfu Fan. 2022. Regionvit: Regional-to-local attention for vision transformers. In *ICLR*.

[6] Mingfei Chen, Yue Liao, Si Liu, Zhiyuan Chen, Fei Wang, and Chen Qian. 2021. Reformulating hoi detection as adaptive set prediction. In *CVPR*.

[7] Alexey Dosovitskiy, Lucas Beyer, Alexander Kolesnikov, Dirk Weissenborn, Xiaohua Zhai, Thomas Unterthiner, Mostafa Dehghani, Matthias Minderer, Georg Heigold, Sylvain Gelly, Jakob Uszkoreit, and Neil Houlsby. 2021. An Image is Worth 16x16 Words: Transformers for Image Recognition at Scale. In *ICLR*.

[8] Hehe Fan, Yi Yang, and Mohan Kankanhalli. 2022. Point spatio-temporal transformer networks for point cloud video modeling. *IEEE TPAMI* (2022).

[9] Hehe Fan, Yi Yang, and Mohan S. Kankanhalli. 2021. Point 4D Transformer Networks for Spatio-Temporal Modeling in Point Cloud Videos. In *CVPR*.

[10] Chen Gao, Jiarui Xu, Yuliang Zou, and Jia-Bin Huang. 2020. DRG: Dual relation graph for human-object interaction detection. In *ECCV*.

[11] Chen Gao, Yuliang Zou, and Jia-Bin Huang. 2018. iCAN: Instance-Centric Attention Network for Human-Object Interaction Detection. In *BMVC*.

[12] Georgia Gkioxari, Ross Girshick, Piotr Dollár, and Kaiming He. 2018. Detecting and recognizing human-object interactions. In *CVPR*.

[13] Yangyang Guo, Zhiyong Cheng, Liqiang Nie, Yibing Liu, Yinglong Wang, and Mohan Kankanhalli. 2019. Quantifying and alleviating the language prior problem in visual question answering. In *SIGIR*.

[14] Yangyang Guo, Zhiyong Cheng, Liqiang Nie, Yinglong Wang, Jun Ma, and Mohan Kankanhalli. 2019. Attentive long short-term preference modeling for personalized product search. *ACM TOIS* (2019).

[15] Saurabh Gupta and Jitendra Malik. 2015. Visual semantic role labeling. *arXiv preprint arXiv:1505.04474* (2015).

[16] Tanmay Gupta, Alexander Schwing, and Derek Hoiem. 2019. No-frills human-object interaction detection: Factorization, layout encodings, and training techniques. In *ICCV*.

[17] Kaiming He, Xiangyu Zhang, Shaoqing Ren, and Jian Sun. 2016. Deep residual learning for image recognition. In *CVPR*.

[18] Zhi Hou, Xiaojiang Peng, Yu Qiao, and Dacheng Tao. 2020. Visual compositional learning for human-object interaction detection. In *ECCV*.

[19] Zhi Hou, Baosheng Yu, Yu Qiao, Xiaojiang Peng, and Dacheng Tao. 2021. Affordance Transfer Learning for Human-Object Interaction Detection. In *CVPR*.

[20] Zhi Hou, Baosheng Yu, Yu Qiao, Xiaojiang Peng, and Dacheng Tao. 2021. Detecting human-object interaction via fabricated compositional learning. In *CVPR*.

[21] Bumsoo Kim, Taeho Choi, Jaewoo Kang, and Hyunwoo J Kim. 2020. UnionDet: Union-level detector towards real-time human-object interaction detection. In *ECCV*.

[22] Bumsoo Kim, Junhyun Lee, Jaewoo Kang, Eun-Sol Kim, and Hyunwoo J Kim. 2021. HOTR: End-to-End Human-Object Interaction Detection with Transformers. In *CVPR*.

[23] Dong-Jin Kim, Xiao Sun, Jinsoo Choi, Stephen Lin, and In So Kweon. 2021. Acp++: Action Co-occurrence Priors for Human-Object Interaction Detection. *IEEE TIP* (2021).

[24] Yong-Lu Li, Xinpeng Liu, Han Lu, Shiyi Wang, Junqi Liu, Jiefeng Li, and Cewu Lu. 2020. Detailed 2d-3d joint representation for human-object interaction. In *CVPR*.

[25] Yong-Lu Li, Xinpeng Liu, Xiaoqian Wu, Yizhuo Li, and Cewu Lu. 2020. HOI Analysis: Integrating and Decomposing Human-Object Interaction. In *NeurIPS*.

[26] Yong-Lu Li, Siyuan Zhou, Xijie Huang, Liang Xu, Ze Ma, Hao-Shu Fang, Yanfeng Wang, and Cewu Lu. 2019. Transferable interactiveness knowledge for human-object interaction detection. In *CVPR*.

[27] Yue Liao, Si Liu, Fei Wang, Yanjie Chen, Chen Qian, and Jiashi Feng. 2020. PPDM: Parallel point detection and matching for real-time human-object interaction detection. In *CVPR*.

[28] Tsung-Yi Lin, Priya Goyal, Ross B. Girshick, Kaiming He, and Piotr Dollár. 2017. Focal Loss for Dense Object Detection. *ICCV*.

[29] Tsung-Yi Lin, Michael Maire, Serge Belongie, James Hays, Pietro Perona, Deva Ramanan, Piotr Dollár, and C Lawrence Zitnick. 2014. Microsoft COCO: Common objects in context. In *ECCV*.

[30] Chunxiao Liu, Zhendong Mao, An-An Liu, Tianzhu Zhang, Bin Wang, and Yongdong Zhang. 2019. Focus your attention: A bidirectional focal attention network for image-text matching. In *ACM MM*.

[31] Fenglin Liu, Xian Wu, Shen Ge, Xiaoyu Zhang, Wei Fan, and Yuexian Zou. 2020. Bridging the gap between vision and language domains for improved image captioning. In *ACM MM*.

[32] Ye Liu, Junsong Yuan, and Chang Wen Chen. 2020. ConsNet: Learning consistency graph for zero-shot human-object interaction detection. In *ACM MM*.

[33] Ze Liu, Yutong Lin, Yue Cao, Han Hu, Yixuan Wei, Zheng Zhang, Stephen Lin, and Baining Guo. 2021. Swin Transformer: Hierarchical Vision Transformer using Shifted Windows. In *ICCV*.

[34] Ilya Loshchilov and Frank Hutter. 2018. Decoupled Weight Decay Regularization. In *ICLR*.

[35] Mandela Patrick, Dylan Campbell, Yuki Markus Asano, Ishan Misra, Florian Metze, Christoph Feichtenhofer, Andrea Vedaldi, and João F. Henriques. 2021. Keeping Your Eye on the Ball: Trajectory Attention in Video Transformers. In *NeurIPS*.

[36] Siyuan Qi, Wenguan Wang, Baoxiong Jia, Jianbing Shen, and Song-Chun Zhu. 2018. Learning human-object interactions by graph parsing neural networks. In *ECCV*.

[37] Zhen Qin, Weixuan Sun, Hui Deng, Dongxu Li, Yunshen Wei, Baohong Lv, Junjie Yan, Lingpeng Kong, and Yiran Zhong. 2022. cosFormer: Rethinking Softmax in Attention. In *ICLR*.

[38] Shaoqing Ren, Kaiming He, Ross Girshick, and Jian Sun. 2015. Faster R-CNN: Towards real-time object detection with region proposal networks. In *NeurIPS*.

[39] Peter Shaw, Jakob Uszkoreit, and Ashish Vaswani. 2018. Self-Attention with Relative Position Representations. In *NAACL (short)*.

[40] Liyue Shen, Serena Yeung, Judy Hoffman, Greg Mori, and Li Fei-Fei. 2018. Scaling human-object interaction recognition through zero-shot learning. In *WACV*.

[41] Masato Tamura, Hiroki Ohashi, and Tomoaki Yoshinaga. 2021. QPIC: Query-Based Pairwise Human-Object Interaction Detection with Image-Wide Contextual Information. In *CVPR*.

[42] Ruijie Tao, Zexu Pan, Rohan Kumar Das, Xinyuan Qian, Mike Zheng Shou, and Haizhou Li. 2021. Is someone speaking? exploring long-term temporal features for audio-visual active speaker detection. In *ACM MM*.

[43] Oytun Ulutan, ASM Iftekhar, and Bangalore S Manjunath. 2020. VSGNet: Spatial attention network for detecting human object interactions using graph convolutions. In *CVPR*.

[44] Ashish Vaswani, Noam Shazeer, Niki Parmar, Jakob Uszkoreit, Llion Jones, Aidan N Gomez, Łukasz Kaiser, and Illia Polosukhin. 2017. Attention is All you Need. In *NeurIPS*.

[45] Oriol Vinyals, Alexander Toshev, Samy Bengio, and Dumitru Erhan. 2016. Show and tell: Lessons learned from the 2015 mscoco image captioning challenge. *IEEE TPAMI* (2016).

[46] Bo Wan, Desen Zhou, Yongfei Liu, Rongjie Li, and Xuming He. 2019. Pose-aware multi-level feature network for human object interaction detection. In *ICCV*.

[47] Tiancai Wang, Tong Yang, Martin Danelljan, Fahad Shahbaz Khan, Xiangyu Zhang, and Jian Sun. 2020. Learning human-object interaction detection using interaction points. In *CVPR*.

[48] Wenxiao Wang, Lu Yao, Long Chen, Deng Cai, Xiaofei He, and Wei Liu. 2022. Crossformer: A versatile vision transformer based on cross-scale attention. In *ICLR*.

[49] Yiling Wu, Shuhui Wang, Guoli Song, and Qingming Huang. 2019. Learning fragment self-attention embeddings for image-text matching. In *ACM MM*.

[50] Bingjie Xu, Junnan Li, Yongkang Wong, Qi Zhao, and Mohan S Kankanhalli. 2019. Interact as you intend: Intention-driven human-object interaction detection. *IEEE TMM* (2019).

[51] Bingjie Xu, Yongkang Wong, Junnan Li, Qi Zhao, and Mohan S Kankanhalli. 2019. Learning to detect human-object interactions with knowledge. In *CVPR*.

[52] Ziwei Xu, Guangzhi Wang, Yongkang Wong, and Mohan S Kankanhalli. 2021. Relation-aware Compositional Zero-shot Learning for Attribute-Object Pair Recognition. *IEEE TMM* (2021).

[53] Hangjie Yuan, Mang Wang, Dong Ni, and Liangpeng Xu. 2022. Detecting Human-Object Interactions with Object-Guided Cross-Modal Calibrated Semantics. In *AAAI*.

[54] Aixi Zhang, Yue Liao, Si Liu, Miao Lu, Yongliang Wang, Chen Gao, and Xiaobo Li. 2021. Mining the Benefits of Two-stage and One-stage HOI Detection. In *NeurIPS*.

[55] Frederic Z Zhang, Dylan Campbell, and Stephen Gould. 2021. Spatially conditioned graphs for detecting human-object interactions. In *ICCV*.

[56] Frederic Z. Zhang, Dylan Campbell, and Stephen Gould. 2022. Efficient Two-Stage Detection of Human-Object Interactions with a Novel Unary-Pairwise Transformer. In *CVPR*.

[57] Xubin Zhong, Xian Qu, Changxing Ding, and Dacheng Tao. 2021. Glance and Gaze: Inferring Action-aware Points for One-Stage Human-Object Interaction Detection. In *CVPR*.

[58] Cheng Zou, Bohan Wang, Yue Hu, Junqi Liu, Qian Wu, Yu Zhao, Boxun Li, Chenguang Zhang, Chi Zhang, Yichen Wei, et al. 2021. End-to-end human object interaction detection with hoi transformer. In *CVPR*.